Appl Phys A (2014) 114:429–434
DOI 10.1007/s00339-013-7626-2

Applied Physics A
Materials Science & Processing

Performance and stability studies of inverted polymer solar cells with TiO_2 film as a buffer layer

Ruixiang Peng · Feng Yang · Xinhua Ouyang · Ying Liu · Yong-Sang Kim · Ziyi Ge

Received: 26 September 2012 / Accepted: 10 February 2013 / Published online: 22 February 2013

Abstract TiO_2 based inverted polymer solar cells (PSCs) with a structure of fluorine-doped tin oxide (FTO)/TiO_2/P3HT:PCBM/PEDOT:PSS/Ag presented excellent air stabilities,; the power conversion efficiency (PCE) of devices exhibited only 15 % decay as compared to the highest value while being exposed in air-condition for more than 20 days. Interestingly, an overall enhancement of PCE from 3.5 % to 3.9 % was observed while the PSCs were exposed in air-condition up to 3 days; the improvement of performance was attributed to the TiO_2 films' oxygen and water protection effect and the oxidation of Ag, which will benefit to form an effective work function match with the HOMO of P3HT leading to improved ohmic contact. However, the performance slowly decreased when the exposure time remains longer due to the physical adsorbed oxygen. UV–ozone treatment on the TiO_2 films' leads to the formation of a metal-deficient oxide that results in a decreased PCE for the devices. Finally, X-ray photo-emission spectroscopy (XPS) was used to analyze the compositional changes of the TiO_2 films while they were exposed in air-condition or treated by UV–ozone.

R. Peng · F. Yang · X. Ouyang · Y. Liu · Z. Ge (✉)
Ningbo Institute of Material Technology & Engineering, Chinese Academy of Sciences, Ningbo 315201, P.R. China
e-mail: geziyi@nimte.ac.cn
Fax: +86-574-86680273

Y.-S. Kim
Department of Electrical Engineering, Myongji University, Gyeonggi 449-728, South Korea

1 Introduction

Extensive efforts have been directed at developing polymer solar cells in the past decades due to their advantages being lightweight, low cost, and flexibility. The performance of the laboratory-scale polymer solar cells based on new donor materials have been demonstrated with power conversion efficiencies up to 7 % in the conventional architecture consisting of a polymer donor and fullerene acceptor blend that is inserted between a high work function ITO anode and a low work function metal cathode [1–3]. However, exposure of these kinds of devices to air can lead to oxidation of the electrode and degradation of the active layer from oxygen and moisture diffusing through grain boundaries and pinholes of the metal electrode [4], which will seriously limit their application. In addition, the deposition of metal leads to metal diffusion through the active layer, which can react with the polymer and alter its semiconducting properties [5, 6]. In order to solve these problems, a new approach was employed by inserting a metal oxide buffer layer between the active layer and ITO anode to reduce the amount of damage and oxygen diffusion into the polymer, called "inverted cells" [7–15].

Recently, a series of metal oxides, such as Cs_2CO_3 [16, 17], ZnO [18–20], and TiO_2 [21, 22] have been extensively used as a buffer layer to overcome these problems and improve device stability. TiO_2 provides a promising alternative because of its high electron mobility and optical transparency, as well as their ease of synthesis. The TiO_2 film also has a substantial oxygen and water protection effect due to the combination of photocatalysis and inherent oxygen deficiency [11, 23, 24], thereby improving the lifetime of unpackaged devices exposed to air. Many demonstrations of using the TiO_2 film as the electron selective layer for inverted polymer solar cells

have been reported. Chen at al. [25] reported a PCE of 2.57 % with a ITO/nc-TiO_2/P3HT:PCBM/MoO_3/Ag device structure. Amorphous titanium oxide was also demonstrated by the Takahashi group [22] as the electron collection electrode inserted between ITO and the active layer with a ITO/TiO_x/PCBM:P3HT/PEDOT:PSS/Au inverted structure; a PCE of 2.47 % was obtained by irradiating at AM 1.5 G. Heeger group [26] introduced a solution-based titanium oxide (TiO_x) as an optical spacer on top of the active layer to improve the PCE of polymer photovoltaic cells. However, the major challenges in using the TiO_2 film as an electron transporting layer are the presence of defects with adsorbed oxygen and poor spatial distribution of the nanoparticles over a large area [27, 28]. In the meanwhile, the degradation mechanism of the polymer solar cells, such as exposure to air, as well as UV-zone treatment have only been partially understood [29, 30].

In this paper, inverted polymer solar cells with a structure of FTO/TiO_2/P3HT:PCBM/PEDOT:PSS/Ag were fabricated. The effects of TiO_2 films interact with atmosphere and UV-light on the stability performance of inverted organic solar cells were investigated. The compositional changes, especially the O/Ti atom concentration ratio of the TiO_2 films, significantly affected the device performance were demonstrated by XPS analysis.

2 Experimental

2.1 Materials and the chemicals

A fluorine-doped tin oxide (FTO) glass sheet (2.2 mm thick, ≤ 14 Ω/square, transmittance >90 %) was purchased from the Nippon Sheet Glass Company, Ltd.; PEDOT:PSS (Baytron® P VP Al 4083) and $PC_{60}BM$ were purchased from Luminescence Chemical Engineering Technology Co., Ltd, tetrabutyl titanate (Acros, 98+ %), dichlorobenzene and hexamethylene disilazane (HMDS) were purchased from Acros. All other reagents were obtained from the Sinopham Chemical Reagent Co., Ltd., and used as received if not specified. P3HT was synthesized following the method described elsewhere; the average molecular mass (Mw) of the synthesized polymer was 32,000 with a polydispersity index of 1.6, as determined with a WATERS 150-C gel permeation chromatography (GPC) with THF as the solvent and monodispersed polystyrene as standard.

2.2 Devices fabrication

In this paper, inverted polymer solar cells with the device structure of fluorine-doped tin oxide (FTO)/TiO_2 films/P3HT:PCBM/PEDOT:PSS/Ag was fabricated; $J-V$ characteristics and XPS analysis were used to investigate the device stability performance after it was exposed to air or UV–ozone environment. To fabricate the solar cells, a composite solution of P3HT and PCBM was prepared using 1,2-dichloro-benzene as the solvent. The concentration of the composite solution was maintained around 30 mg/mL with 1 % (v/v) 1,8-octanedithiol. The inverted polymer solar cells with the sandwich structure FTO/TiO_2/P3HT:PCBM/PEDOT:PSS/Ag were fabricated. The TiO_2-sol was prepared following the previously reported method [25] and then spin coated on cleaned FTO substrates (1 inch × 1 inch), which were cleaned by a routine cleaning procedure that consisted of washing in an aqueous detergent, and then sequential sonication in acetone, isopropanol, and deionized water, and finally rinsed with ethanol and dried in a N_2 stream. The TiO_2 layer was sintered at 500 °C for 1 h under ambient conditions. Their thickness of TiO_2 film was about 40 nm. The predissolved composite solution was filtered through a 0.45 μm syringe filter and an active layer of ~300 nm was spin coated on the TiO_2 layer. Subsequently, hexamethylene disilazane (HMDS) was precoated immediately onto the active layer. PEDOT:PSS mixed with 1 % (v/v) of Triton X-100 ($C_{14}H_{22}O(C_2H_4O)n$) nonionic surfactant was spin-coated onto the surface of the active layer. Thermal preannealing was conducted at 120 °C for 30 min on a hot plate in a glovebox (MBRAUN, $H_2O \leq 0.1$ ppm, $O_2 \leq 0.1$ ppm). Finally, a cathode (top electrode) of Ag was deposited onto the PEDOT:PSS layer in a thermal evaporator (MB-EVAP) under a vacuum of 5×10^{-7} mbar.

2.3 Characterization

The thickness of films was measured using surface profiler (Dektak 150). The current-voltage (I-V) characteristics of all the photovoltaic cells were measured under the simulated solar light (100 mW/cm^2; AM 1.5 G) provided by Newport-Oriel® Sol3A 1000-W solar simulator. Electrical data were recorded using a Keithley 2440 source-measure unit. The intensity of the simulated solar light was calibrated by a standard Si photodiode detector (PV measurements Inc.), which was calibrated at NREL. The Al Ka radiation source ($hv = 1486.6$ eV) was used for the XPS (Kratos AXIS ULTRA^{DLD}) characterization.

3 Results and discussion

3.1 Device performance affected by exposing in air condition

Figure 1 shows the correlation between the exposure time and PCE of the inverted PSCs with devices structure of FTO/TiO_2 films/P3HT:PCBM/PEDOT:PSS/Ag, devices were exposed in air-condition without any other protection for more than 20 days and characterized under AM

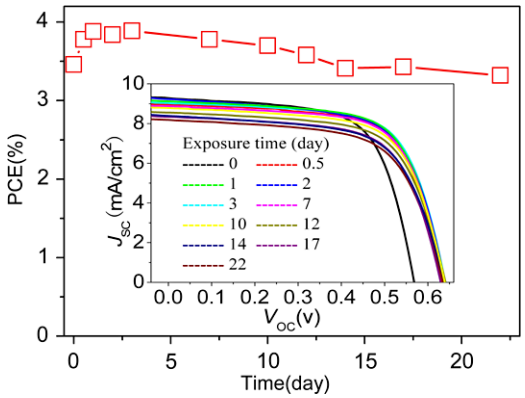

Fig. 1 PCE of the inverted PSCs exposed in air-condition for various times. The *inset figure* shows the J–V curves which were tested under illumination of 100 mW/cm^2

Table 1 Photovoltaic performance of the inverted PSCs for various times

Exposure time (d)	V_{OC} (V)	J_{SC} (mA/cm^2)	FF (%)	R (at V_{OC})	PCE (%)
0	0.57	9.3	66	65	3.5
0.5	0.63	9.0	67	71	3.8
1	0.64	9.1	67	74	3.9
2	0.64	9.2	65	73	3.8
3	0.64	9.0	67	72	3.9
7	0.64	8.9	67	77	3.8
10	0.64	8.8	66	76	3.7
12	0.64	8.6	65	87	3.6
14	0.64	8.4	64	94	3.4
17	0.63	8.3	65	80	3.4
22	0.63	8.2	64	92	3.3

1.5 G simulated solar illumination of 100 mW/cm^2. The inset figure shows the current density–voltage (J–V) curves of the device. To get a better understanding, performances of the inverted PSC photovoltaic are listed in Table 1. As depicted in Fig. 1, the inverted device exhibits an original PCE of 3.5 %, with $J_{SC} = 9.3$ mA/cm^2, $V_{OC} = 0.57$, and FF = 65 %. While the device was exposed to air-condition, the V_{OC} remarkably increased from the original value of 0.57 V to 0.64 V. Furthermore, the PCE increased to the highest value of 3.9 % after exposing to air for 3 days with $J_{SC} = 9.0$ mA/cm^2, $V_{OC} = 0.64$, and FF = 67 %, and then slowly decreased to 3.3 %, with $J_{SC} = 8.2$ mA/cm^2, $V_{OC} = 0.63$, and FF = 64 %. The results present excellent air stabilities; even the devices were exposed in a natural environment for more than 20 days, the PCE is still about 95 % compared to the original value, and an overall performance enhancement with PCE from 3.5 to 3.9 % was observed while exposing the PSCs in air-condition for 3 days. However, the efficiency slowly decreased when the exposure time remains longer. In consideration of that photo-oxidation of the active layers in air condition or even degradation of the top PEDOT:PSS is unbeneficial for the PSCs stabilities. Similar results were also observed by Kang et al. [31] and White et al. [32] of using ZnO as the electron selective layer and an Ag electrode as the top hole collecting layer in inverted polymer solar cells. They attributed the improvement of V_{OC} to the oxidation of Ag. In the case of the Ag electrode, the oxidization of Ag will increase its work function from 4.3 to 5.0 eV, which will benefit to form an effective work function match with the HOMO of P3HT leading to an improved ohmic contact. However, the oxidization of Ag will increase its resistance, which is not beneficial for the electron transfer. Atomic concentrations of oxygen and titanium also play an important role in the photovoltaic performance of the TiO_2 based inverted PSCs due to the inherent oxygen deficiency in which the dominant defects in TiO_2 are oxygen vacancies, which will significantly affect its conductivity [24, 33]. Trap-filling in the TiO_2 film by photogenerated charges leads to increased photoconductivity [21]. The reduction of the PCE for the device exposed in air-condition for a very long time was attributed to the presence of defects with physical adsorbed oxygen [34–36], which increased the contact resistance between the TiO_2 film and active layer resulting in a decreased overall performance.

3.2 UV–ozone treatment

To further investigate the effect of TiO_2 films' compositional changes on the performance of the inverted PSCs, we performed a UV–ozone treatment on the TiO_2 films. Previous work has shown that the UV–ozone treatment can tune the oxygen concentration, but not alter the TiO_2 nanoparticle size, shape, or distribution of the nanoclusters in the films [23]. The J–V characteristics of the inverted PSCs with UV–ozone exposure on TiO_2 films for various duration are shown in Fig. 2. All the devices were tested under AM 1.5 G simulated solar illumination of 100 mW/cm^2. The TiO_2 films were UV–ozone treated for 10, 30, 60, and 120 min, respectively, leading to the obvious decrease in the J_{SC}, FF, and PCE values for the inverted $PC_{61}BM$/P3HT solar cells compared to cells without a UV–ozone treatment. Detailed photovoltaic parameters are presented in Table 2. We can observe that the device without the UV-zone treatment exhibits a PCE of 3.4 %, with $J_{SC} = 9.3$ mA/cm^2, $V_{OC} = 0.57$, and FF = 65 %, while the UV–ozone treated TiO_2 films for 30 min led to a PCE of 3.1 %, with $J_{SC} = 9.1$ mA/cm^2, $V_{OC} = 0.56$, and FF = 61 %. For devices with TiO_2 films that has been UV–ozone treated for more than 30 min, a reduction of J_{SC} and FF were observed. UV–ozone treated TiO_2 films for 120 min led to a PCE of 2.6 %, with $J_{SC} = 8.2$ mA/cm^2, $V_{OC} = 0.56$, and FF = 58 %. The PCE is only 76 % compared to the original value. As illustrated, the UV–ozone treatment of the TiO_2 films leads to a decreased de-

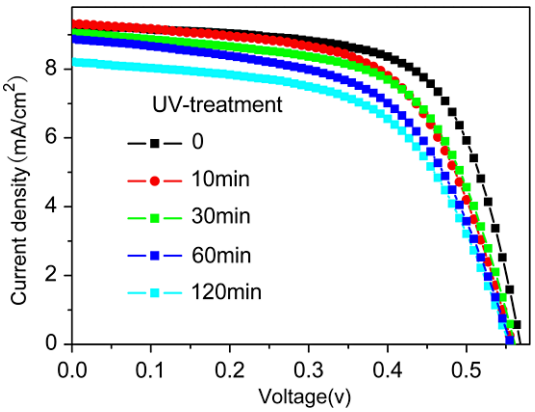

Fig. 2 J–V curves of inverted PSCs with UV–ozone treatment for various times (0, 10, 30, 60, and 120 min) under illumination of 100 mW/cm^2

Table 2 Photovoltaic performance of the inverted PSCs with UV–ozone treatment

UV-zone treatment	V_{OC} (V)	J_{SC} (mA/cm^2)	FF (%)	R (at V_{OC})	PCE (%)
0	0.57	9.3	65	69	3.4
10 min	0.56	9.3	60	95	3.1
30 min	0.56	9.1	61	90	3.1
60 min	0.56	8.7	57	112	2.8
120 min	0.55	8.2	58	123	2.6

vice performance. TiO_2 is well known that a nonstoichiometric compound, which has been generally considered as an oxygen-deficient compound, TiO_{2-x}. However, strong oxidation of TiO_2 through the UV–ozone treatment leads to the formation of a metal-deficient oxide [37, 38]. In this case, TiO_2 may be represented by the formula $Ti_{1-x}O_{2-y}$, where $x > y/2$. The properties of the metal deficient TiO_2 are determined by titanium vacancies, which are formed during a prolonged oxidation process, in consequence, leading to a formation of electron trapping due to the reduction of titanium vacancies that reduces the electron extraction efficiency between TiO_2 and active layer.

3.3 Compositional study using XPS

To confirm the compositional changes, X-ray photo-emission spectroscopy (XPS) was performed on the TiO_2 film samples. The XPS spectra (Fig. 3) for C 1s, O 1s, and Ti 2p were measured for (a) as-prepared, (b) UV–ozone treated for 30 min, and (c) air exposed for 2 days in air-condition, respectively. The binding energies were calibrated by taking the C 1s peak (284.6 eV) as a reference. The O 1s XPS spectra for three TiO_2 films are shown in Fig. 3(a). The UV–ozone treatment and exposure in air-condition increased the relative magnitude of the peak at ~531.7 eV (corresponding to the oxygen atoms bonded to the titanium in the TiO_2

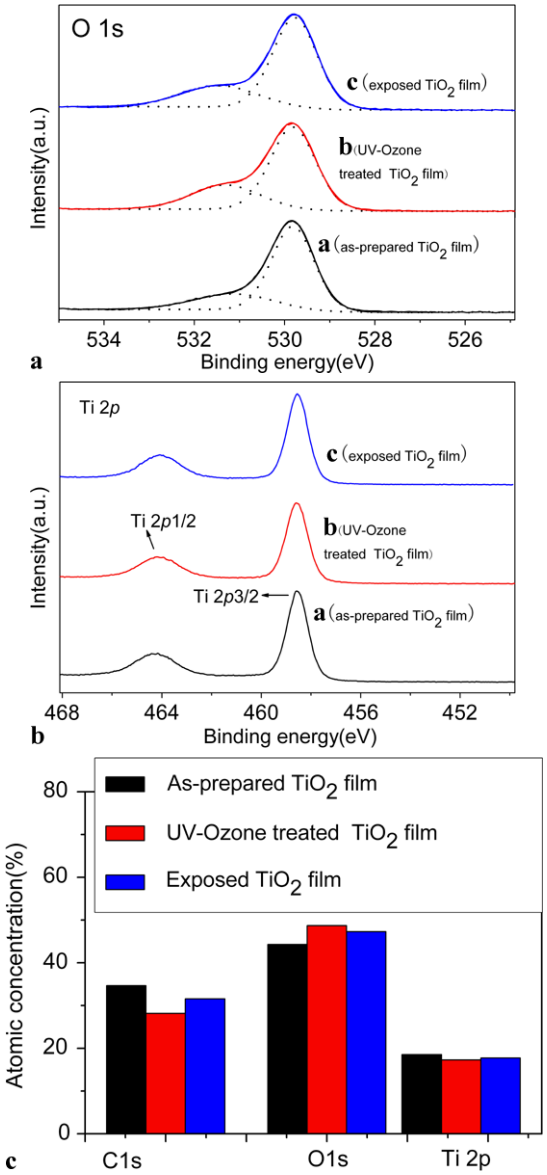

Fig. 3 XPS data for the as-prepared, 30 min UV–ozone and air–condition exposed TiO_2 films, respectively (**a**) O 1s, (**b**) Ti 2p, and (**c**) atomic concentration of carbon, oxygen, titanium for TiO_2 films

matrix), and the UV–ozone treatment and exposure in air-condition also increased the relative magnitude of the peak at ~530.1 eV, which corresponds to O^{2-} ions present in the clusters [39–41]. Figure 3(b) shows the Ti 2p XPS spectra for three TiO_2 films. The intensity of the peaks which corresponds to Ti–O bonds of Ti 2p3/2 and Ti 2p1/2 decreased at 458.7 and 464.5 eV [42], respectively. The results are in agreement with that for the O 1s spectra. The atomic concentrations of carbon, oxygen, and titanium of the as-prepared, UV–ozone treated, and air exposed TiO_2 films based on the C 1s, O 1s, and Ti 2p XPS spectra are summarized in Fig. 3(c). The result shows that the atomic concentration of carbon for the TiO_2 film is obviously reduced

by the UV–ozone treatment. The relative atomic concentrations ratio of oxygen atom compared to Titanium (O/Ti) for three TiO_2 films is 2.39 of the as-prepared TiO_2 film, 2.82 of the UV–ozone treated TiO_2 film, and 2.66 of the exposed TiO_2 film, respectively. The UV–ozone treated TiO_2 film presented the highest value of O/Ti, which confirmed the formation of a metal-deficient oxide, in consequence, significantly decreased the electron extraction efficiency of the devices. According to the $J–V$ characterization, we conclude that a short time exposure treatment in air-condition lead to a light increase of relative atomic concentration of O/Ti, the improvement of PCE after exposing devices to the air condition for 2 days was attributed to the effect of the oxidation of Ag, which will improve the V_{OC} due to the increased ohmic contact between the TiO_2 film and active layer. and also the filling of oxygen vacancies, which will significantly increase its photoconductivity. However, long time exposure makes the nanocomposite TiO_2 films become oxygen-rich, which reduces the electron extraction efficiency resulting in a decreased PCE.

4 Conclusion

In conclusion, the TiO_2 based inverted polymer solar cells with the device structure of FTO/TiO_2 films/P3HT:PCBM/PEDOT:PSS/Ag exhibit excellent air stabilities. A highest PCE of 3.9 % was presented with $J_{SC} = 9.0$ mA/cm^2, $V_{OC} = 0.64$, FF = 67 %. The performance of devices exhibited only 15 % decay as compared to the highest value while being exposed in air-condition for more than 20 days, while the devices were exposed in air for a longer time. The performance slowly decreased due to the physical adsorbed oxygen, which increased contact resistance between the TiO_2 film and active layer. The UV–ozone treatment on the TiO_2 films' lead to the formation of a metal-deficient oxide that is not beneficial for the devices performance.

Acknowledgements This work was financially supported from the National Natural Science Foundation of China (21074144), the Fok Ying-Tong Education Foundation (122027), Qianjiang Telent Project, and visiting professorship for Senior International Scientists from the Chinese Academy of Science.

References

1. Y.Y. Liang, L.P. Yu, Acc. Chem. Res. **43**, 1227 (2010)
2. H.-Y. Chen, J.H. Hou, S.Q. Zhang, Y.Y. Liang, G.W. Yang, Y. Yang, L.P. Yu, Y. Wu, G. Li, Nat. Photonics **3**, 649 (2009)
3. C.E. Small, S. Chen, J. Subbiah, C.M. Amb, S.W. Tsang, T.H. Lai, J.R. Reynolds, F. So, Nat. Photonics **6**, 115 (2011)
4. F.C. Krebs, K. Norrman, Prog. Photovolt. **15**, 697 (2007)
5. M. Boman, S. Stafstrom, J.L. Bredas, J. Chem. Phys. **97**, 12 (1992)
6. J. Birgerson, M. Fahlman, P. Broms, W.R. Salaneck, Synth. Met. **80**, 125 (1996)
7. H. Schmidt, H. Flügge, T. Winkler, T. Bülow, T. Riedl, W. Kowalsky, Appl. Phys. Lett. **94**, 243302 (2009)
8. W.H. Baek, M.J. Choi, T.S. Yoon, H.H. Lee, Y.S. Kim, Appl. Phys. Lett. **96**, 133506 (2010)
9. J.H. Huang, H.Y. Wei, K.C. Huang, C.L. Chen, R.R. Wang, F.C. Chen, K.C. Ho, C.W. Chu, Energy Environ. Sci. **3**, 654 (2010)
10. S.K. Hau, H.L. Yip, N.S. Baek, J. Zou, K.O. Malley, A.K.Y. Jen, Appl. Phys. Lett. **92**, 253301 (2008)
11. K. Lee, J.Y. Kim, S.H. Park, S.H. Kim, S. Cho, A.J. Heeger, Adv. Mater. **19**, 2445 (2007)
12. F.J. Zhang, X.W. Xu, W.H. Tang, J. Zhang, Z.L. Zhuo, J. Wang, J. Wang, Z. Xu, Y.S. Wang, Sol. Energy Mater. Sol. Cells **95**, 1785 (2011)
13. K. Steven, H.-L. Hau, Y. Alex, K.-Y. Jen, Polym. Rev. **50**, 474 (2010)
14. P. Riccardo, C. Chiara, B. Andrea, C. Nadia, Energy Environ. Sci. **4**, 285 (2011)
15. H. Ma, H.-L. Yip, F. Huang, A.K.-Y. Jen, Adv. Funct. Mater. **20**, 1371 (2010)
16. Y.F. Lim, S. Lee, D.J. Herman, M.T. Lloyd, J.E. Anthony, G.G. Malliaras, Appl. Phys. Lett. **93**, 193301 (2008)
17. C. Waldauf, M. Morana, P. Denk, P. Schilinsky, K. Coakley, S.A. Choulis, C.J. Brabec, Appl. Phys. Lett. **89**, 233517 (2006)
18. S.K. Hau, H.L. Yip, K. Leong, A.K.Y. Jen, Org. Electron. **10**, 719 (2009)
19. S.K. Hau, H.L. Yip, J. Zou, A.K.Y. Jen, Org. Electron. **10**, 1401 (2009)
20. M.A. Ibrahem, H.-Y. Wei, M.-H. Tsai, K.-C. Ho, J.-J. Shyue, C.W. Chu, Sol. Energy Mater. Sol. Cells **108**, 156 (2013)
21. H. Schmidt, K. Zilberberg, S. Schmale, H. Flügge, T. Riedl, W. Kowalsky, Appl. Phys. Lett. **96**, 243305 (2010)
22. T. Kuwabara, T. Nakayama, K. Uozumi, T. Yamaguchi, K. Takahashi, Sol. Energy Mater. Sol. Cells **92**, 1476 (2008)
23. Y.J. Cheng, F.Y. Cao, W.C. Lin, C.H. Chen, C.H. Hsieh, Chem. Mater. **23**, 1512 (2011)
24. L. Linsebigler, G. Lu, J.T. Yates, Chem. Rev. **95**, 735 (1995)
25. C. Tao, S.P. Ruan, X.D. Zhang, G.H. Xie, L. Shen, X.Z. Kong, W. Dong, C.X. Liu, W.Y. Chen, Appl. Phys. Lett. **93**, 193307 (2008)
26. J.Y. Kim, S.H. Kim, H.-H. Lee, K. Lee, W. Ma, X. Gong, A.J. Heeger, Adv. Mater. **18**, 572 (2006)
27. S. Sakohara, M. Ishida, M.A. Anderson, J. Phys. Chem. B **102**, 10169 (1998)
28. S. Monticone, R. Tufeu, A.V. Kanaev, J. Phys. Chem. B **102**, 2854 (1998)
29. D.M. Tanenbaum, M. Hermenau, E. Voroshazi, M.T. Lloyd, Y. Galagan, B. Zimmermann, M. Hosel, H.F. Dam, M. Jørgensen, S.A. Gevorgyan, S. Kudret, W. Maes, L. Lutsen, D. Vanderzande, U. Wurfel, R. Andriessen, R. Rosch, H. Hoppe, G.T. Escobar, M.L. Cantu, A. Rivaton, G.Y. Uzunoglu, D. Germack, B. Andreasen, M.V. Madsen, K. Norrmany, F.C. Krebs, RSC Adv. **2**, 882 (2012)
30. X. Wang, C. Zhao, G. Xu, Z.K. Chen, F. Zhu, Sol. Energy Mater. Sol. Cells **104**, 1 (2012)
31. J.W. Kang, Y.J. Kang, S. Jung, M. Song, D.G. Kim, C. Su, S. Kim, H. Kim, Sol. Energy Mater. Sol. Cells **103**, 76 (2012)
32. M.S. White, D.C. Olson, S.E. Shaheen, N. Kopidakis, D.S. Ginley, Appl. Phys. Lett. **87**, 143517 (2006)
33. M.K. Nowotny, L.R. Sheppard, T. Bak, J. Nowotny, J. Phys. Chem. C **112**, 14 (2008)
34. H. Seemann, J. Egelhaaf, C.J. Brabec, J.A. Hauch, Org. Electron. **10**, 1424 (2009)
35. M.O. Reese, A.J. Morfa, M.S. White, N. Kopidakis, S.E. Shaheen, G. Rumbles, D.S. Ginley, Sol. Energy Mater. Sol. Cells **92**, 746 (2008)
36. L. Lüer, H.J. Egelhaaf, D. Oelkrug, G. Cerullo, G. Lanzani, B.H. Huisman, D. Leeuw, Org. Electron. **5**, 83 (2004)

37. M.K. Nowotny, T. Bak, J. Nowotny, J. Phys. Chem. B **110**, 16302 (2006)
38. J. Nowotny, T. Bak, T. Burg, Int. J. Ion. **13**, 71 (2007)
39. C. Aliaga, J.Y. Park, Y. Yamada, H.S. Lee, C.K. Tsung, P.D. Yang, G.A. Somorjai, J. Phys. Chem. C **113**, 6150 (2009)
40. Y. Masuda, Y. Jinbo, T. Yonezawa, K. Koumoto, Chem. Mater. **14**, 1236 (2002)
41. Z. Tan, W.Q. Zhang, Z.G. Zhang, D.P. Qian, Y. Huang, J.H. Hou, Y.F. Li, Adv. Mater. **24**, 1476 (2012)
42. C.D. Wagner, L.H. Gale, R.H. Raymond, Anal. Chem. **51**, 466 (1979)